

## Luttinger liquid in a finite one-dimensional wire with box-like boundary conditions

Fabrizio Anfuso<sup>1,2</sup> and Sebastian Eggert<sup>1</sup>

<sup>1</sup>*Institute of Theoretical Physics, Chalmers University of Technology and Göteborg University, S-412 96 Göteborg, Sweden*

<sup>2</sup>*Physics Department, University of Bologna, INFN and INFN, I-40127 Bologna, Italy*

(Received 26 August 2003; published 8 December 2003)

We study a Luttinger Liquid in a finite one-dimensional wire with box-like boundary conditions by considering the local distribution of the single-particle spectral weight. This corresponds to the experimental probability of extracting a single electron at a given place and energy, which can be interpreted as the square of an electron wave function. For the noninteracting case, this is given by a standing wave at the Fermi wave vector. In the presence of interactions, however, the wave functions obtain additional structure with a sharp depletion near the edges and modulations throughout the wire. In the spinful case, these modulations correspond to the separate spin- and charge-like excitations in the system.

DOI: 10.1103/PhysRevB.68.241301

PACS number(s): 73.21.Hb, 71.10.Pm, 73.63.-b, 73.22.-f

The problem of a particle in a one-dimensional box is a classic example in almost any quantum mechanics text book since it gives a pedagogical introduction to the concept of energy quantization and provides a complete visualization of the corresponding wave functions. It is however only recently that this problem has gained true experimental relevance due to the progress in constructing smaller and more refined structures to confine electrons in dots and wires. It is, for example, now possible to resolve the electron wave functions in a finite piece of carbon nanotube by scanning tunneling microscopy (STM) experiments.<sup>1-3</sup> Most experimental realizations of one-dimensional electron boxes contain many electrons in a Fermi sea, but it is possible to study a single particle excitation on top of such a ground-state configuration and classify the possible energy levels and wave functions.

However, electron-electron interactions may produce interesting effects in such one-dimensional many-body systems and systematically change the shape of the electron wave-functions. In fact single-particle excitations are no longer the eigenstates of an interacting Hamiltonian, but of course it is still interesting to determine the probability of extracting or inserting individual electrons at a given position and energy. This local probability density can be interpreted as the square of the electron wave function. We therefore study the fundamental problem of single-particle excitations in a many-body *interacting* fermion system confined to a one-dimensional box using the Luttinger Liquid formalism.

We find that the classic example of a box provides again a good visualization of the effect of interactions on the wave function and the energy quantization. In particular, in addition to the expected rapid Fermi wave vector oscillations in the wave-function we can recognize long wavelength modulations, which correspond to the underlying boson-like excitations in the Luttinger liquid. For repulsive interactions the wave-functions are sharply depleted at the edges with a characteristic power law. Analytic expressions for the wave functions of the first few levels are presented. For an analysis of an interacting boson system see Ref. 4.

The Luttinger liquid formalism is a well-established tool to describe interacting electrons confined to one dimension.

<sup>5,6</sup> In a linearized region around the Fermi points the fermion field can be expanded in terms of left and right movers

$$\Psi(x,t) \approx e^{ik_F x} \psi_R(x,t) + e^{-ik_F x} \psi_L(x,t). \quad (1)$$

The Fourier modes of the left- and right-moving fermion density are then represented by bosonic creation and annihilation operators, which effectively act by “shifting” fermions  $m$  steps up or down the spectrum. In the presence of interactions it is then possible to solve the model by a Bogoliubov transformation which mixes the left- and right-moving bosons. This transformation can be described by a single “Luttinger liquid parameter”  $g$ , which gives the hyperbolic cosine  $\alpha$  and sine  $\beta$  of the Bogoliubov transformation

$$\alpha = \frac{1}{2} \left( \frac{1}{g} + g \right), \quad \beta = \frac{1}{2} \left( \frac{1}{g} - g \right). \quad (2)$$

Here  $g < 1$  for repulsive backscattering interactions and  $g = 1$  for no interactions. Forward scattering does not affect this parameter, but rescales the effective Fermi velocity.

Let us now consider spinless fermions in a one-dimensional box of length  $L$  with fixed boundary conditions  $\Psi(0) = \Psi(L) = 0$ . After bosonization the fermion fields become exponentials of the boson operators in a linearized region around the Fermi points

$$\psi_R(x,t) = \frac{1}{\sqrt{2\pi a}} e^{i\sqrt{4\pi}(\alpha\phi_R(x,t) - \beta\phi_L(x,t))}, \quad (3)$$

$$\psi_L(x,t) = \frac{1}{\sqrt{2\pi a}} e^{-i\sqrt{4\pi}(\alpha\phi_L(x,t) - \beta\phi_R(x,t))}, \quad (4)$$

where  $a$  is a short-distance cutoff parameter. The fixed boundary condition therefore relates the left- and right-moving boson fields  $\phi_R(x,t) = -\phi_L(-x,t) + \phi_0$  and determines the mode expansion in terms of ordinary boson creation and annihilation operators, and zero modes<sup>7,8</sup>

$$\phi_L(x,t) = \frac{\phi_0 + \tilde{\phi}_0}{2} + Q \frac{x+vt}{2L} + \sum_{m=1}^{\infty} \frac{1}{\sqrt{4\pi m}} (e^{-i(m\pi/L)(x+vt)} a_m + \text{H.c.}), \quad (5)$$

where  $[\tilde{\phi}_0, Q] = i$  and  $\phi_0 = \sqrt{\pi/2}g$ . The eigenvalues of the zero modes  $Q = (n - n_0 - \frac{1}{2})\sqrt{\pi}/g$  are quantized with the number of electrons  $n$ , where  $n_0 = k_F L / \pi$  corresponds to the number of electrons in the ground state.

The Hamiltonian is given by  $H = (\pi v/L) \sum_m m a_m^\dagger a_m + (v/2L) Q^2$ , where  $v$  is the renormalized Fermi velocity. We see that the last term in  $H$  resembles a ‘‘charging’’ energy proportional to the square of the excess number of fermions, but this will not affect our calculations since we always consider single-particle excitations with exactly one additional fermion  $n = n_0 + 1$ . In general there may also be an additional capacitive energy with a corresponding single-particle charging energy  $E_0$ .

The boson excitations become highly degenerate with increasing energy levels which are always quantized  $\omega_m = m(\pi v/L)$ . However, we are interested in the corresponding *fermion* wave function of a single-particle excitation on the ground state  $\langle \omega_m | x \rangle = \langle \omega_m | \Psi^\dagger(x) | 0 \rangle$ . The probability density  $\rho(\omega_m, x)$  is given by the sum of the corresponding degenerate wave functions  $\langle \omega_m | x \rangle$  squared

$$\rho(\omega_m, x) \equiv \sum_{\lambda} |\langle \omega_m, \lambda | \Psi^\dagger(x) | 0 \rangle|^2. \quad (6)$$

This is the local density of states which gives the experimental probability of tunneling an electron into the system at energy  $\omega_m$  and position  $x$ . This spectral density can be readily evaluated for an equally spaced spectrum by the Fourier transformation of Green’s function

$$\rho(\omega_m, x) = \frac{v}{2L} \int_0^{2L/v} dt e^{i\omega_m t} \langle \Psi(x, t) \Psi^\dagger(x, 0) \rangle. \quad (7)$$

After defining a ‘‘mixed wave’’  $\chi_m(x) = \alpha e^{im(\pi x/L)} + \beta e^{-im(\pi x/L)}$ , we find

$$\begin{aligned} \langle \psi_L(x, t) \psi_L^\dagger(x, 0) \rangle &= c \left( \sin \frac{\pi x}{L} \right)^{2\alpha\beta} \\ &\times \exp \left[ \sum_{k=1}^{\infty} \frac{e^{-ik(\pi v t/L)}}{k} |\chi_k(x)|^2 \right], \end{aligned} \quad (8)$$

$$\begin{aligned} \langle \psi_R(x, t) \psi_L^\dagger(x, 0) \rangle &= -c \left( \sin \frac{\pi x}{L} \right)^{2\alpha\beta} \\ &\times \exp \left[ \sum_{k=1}^{\infty} \frac{e^{-ik(\pi v t/L)}}{k} \chi_k^2(x) \right]. \end{aligned} \quad (9)$$

Here  $c = (4^{2\alpha\beta}/L)(2\pi a/L)^{2\beta^2}$  is a nonuniversal cutoff-dependent renormalization parameter which sets the units in our calculations and suppresses the spectral weight in the

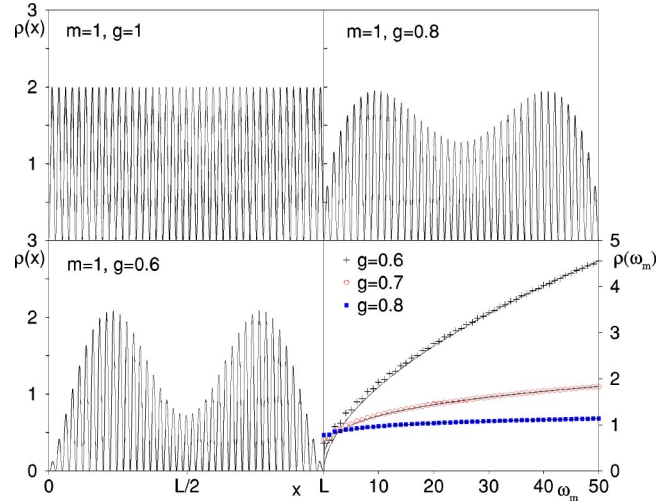


FIG. 1. (Color online) The wave function squared corresponding to  $m=1$  and  $n_0=40$  in units of  $c$ . The modulations become more pronounced with increasing interaction strength (smaller  $g$ ). Last panel: the integrated probability density for the first 50 levels compared to the power law behavior  $\omega^{2\beta^2}$ .

presence of interactions. These correlation functions can be simplified to power laws of sine functions<sup>7–9</sup> but the form above avoids any singularities in the integral of Eq. (7) since for a given level  $\omega_m$  we can truncate the sum in the exponential by  $k \leq m$ . For the first few levels we are even able to evaluate  $\rho$  analytically:

$$\rho(\omega_1, x) = c \left( \sin \frac{\pi x}{L} \right)^{2\alpha\beta} 2 \text{Im}^2[\chi_1(x) e^{ik_F x}],$$

$$\begin{aligned} \rho(\omega_2, x) &= c \left( \sin \frac{\pi x}{L} \right)^{2\alpha\beta} (\text{Im}^2[\chi_1^2(x) e^{ik_F x}] \\ &+ \text{Im}^2[\chi_2(x) e^{ik_F x}]), \end{aligned}$$

$$\begin{aligned} \rho(\omega_3, x) &= c \left( \sin \frac{\pi x}{L} \right)^{2\alpha\beta} \left( \frac{1}{3} \text{Im}^2[\chi_1^3(x) e^{ik_F x}] \right. \\ &+ \text{Im}^2[\chi_1(x) \chi_2(x) e^{ik_F x}] + \frac{2}{3} \text{Im}^2[\chi_3(x) e^{ik_F x}] \Big). \end{aligned} \quad (10)$$

The probability density shows an oscillation of  $2k_F x$  with modulations according to the mixing of left- and right-moving components in  $\chi_m$ . As can be seen in Fig. 1, the amplitude of the modulations increases with the interaction strength (smaller  $g$ ) and the envelope shows a depletion near the edges with a characteristic power law  $x^{2\alpha\beta}$  in agreement with the notion of a boundary exponent.<sup>7–10</sup> In the limit of small level spacing  $L \rightarrow \infty$  we recover the known Luttinger liquid power law behavior of the integrated density of states  $\rho(\omega) \propto \omega^{2\beta^2}$  (last panel of Fig. 1). In Fig. 2 we see that the modulations of level  $\omega_m$  always have  $m$  ‘‘nodes’’ and  $m+1$

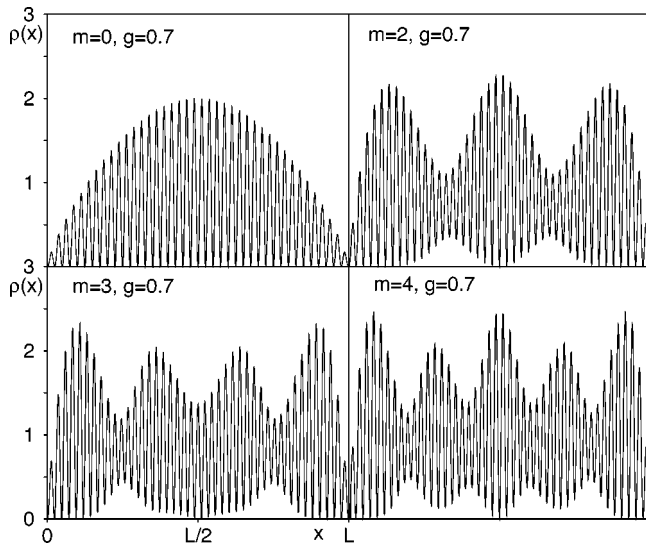


FIG. 2. The wave function squared of the first few levels for  $g=0.7$  and  $n_0=40$  in units of  $c$ .

maxima with roughly equal spacing and height resembling a standing wave with a small wave vector  $\omega_m/v$ , corresponding to the density waves from the boson excitations relative to the Fermi-energy. It is also instructive to consider the noninteracting limit  $g=1$ , for which we always recover a normalized standing wave of wave vector  $2(k_F + \omega_m/v)$  without any modulations or depletion, even though a general single fermion excitation still corresponds to a superposition of degenerate many-boson states (and vice versa).

It is now interesting to explore this modulation pattern for the spinful case where we expect separate spin- and charge-like excitations. In this case the electron field with spin  $\sigma = \pm$  is expressed in terms of spin and charge boson operators with two Luttinger liquid parameters  $g_s$  and  $g_c$ ,

$$\psi_{R,\sigma}(x) = \frac{1}{\sqrt{2\pi a}} e^{i\sqrt{2\pi}(\alpha_c \phi_{R,c} - \beta_c \phi_{L,c})} e^{i\sigma\sqrt{2\pi}(\alpha_s \phi_{R,s} - \beta_s \phi_{L,s})}, \quad (11)$$

and the analogous expression for  $\psi_{L,\sigma}$ . The mode expansions for the spin and charge bosons are the same as in Eq. (5), and the Hamiltonian is also given by the a simple sum  $H = \sum_{\nu=c,s} (\sum_{m_\nu} (v_\nu \pi/L) m_\nu a_{m_\nu}^\dagger a_{m_\nu} + (v_\nu Q_\nu^2/2L))$ . Therefore, the spin and charge excitations are decoupled except for the quantization conditions on the zero modes  $Q_s = (\sqrt{\pi}/\sqrt{2}g_s)l$ ,  $Q_c = (\sqrt{\pi}/\sqrt{2}g_c)[n-1-2k_F L/\pi]$  that  $[l,n]$  must be either both even or both odd ( $[1,1]$  in our case). For the noninteracting case, spin and charge excitations are exactly degenerate, but now the excitations are classified by the product space of two evenly spaced boson spectra with different energy spacing  $v_s < v_c$ . The partition function and the electron Green's function factorize. Therefore, the wave functions are products of spin and charge modulations which are similar to the ones shown in Fig. 2 and Eq. (10), except that the mixed wave is re-

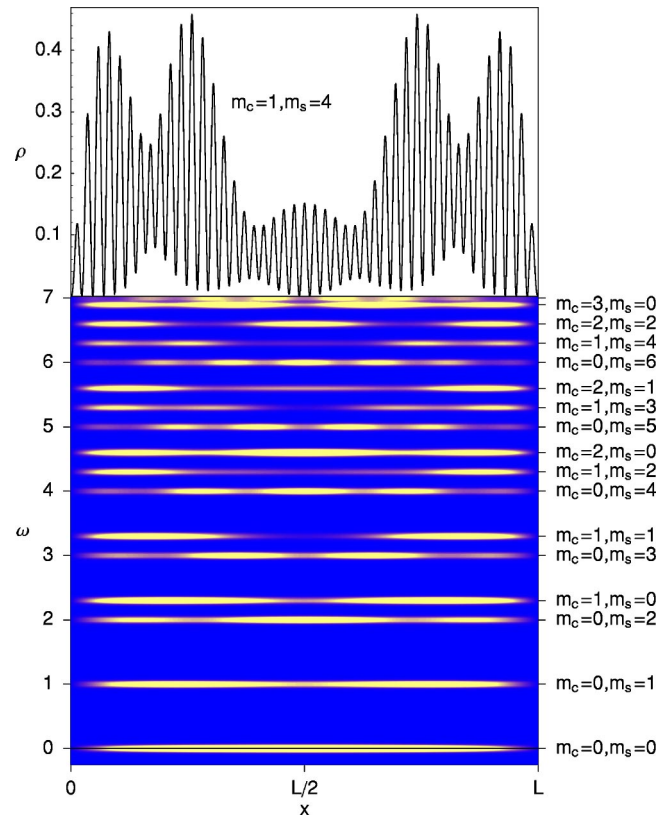


FIG. 3. (Color online) The single-particle density of a spinful interacting electron system as a function of energy and position along a finite box for  $g_s=0.7$ ,  $g_c=0.6$ , and  $v_c=2.3v_s$  (slightly broadened, so that the fast oscillations are averaged out). This may resemble the outcome of a  $dI/dV$  measurement in a STM experiment on a finite interacting wire. Top: fully resolved level for  $m_s=4, m_c=1$ , and  $(k_F L/\pi)=40$ . The two charge peaks and the five weaker spin peaks are visible.

scaled  $\chi_{m,\nu}(x) = (\alpha_\nu/\sqrt{2})e^{im(\pi x/L)} + (\beta_\nu/\sqrt{2})e^{-im(\pi x/L)}$ ,  $\nu = s, c$ , and the overall factor is given by  $[\sin(\pi x/L)]^{\alpha_s \beta_s} [\sin(\pi x/L)]^{\alpha_c \beta_c}$ .

In Fig. 3 we show the square of the wave functions at the lowest energies in a spinful interacting electron system with  $g_s=0.7, g_c=0.6$ , and  $v_c=2.3v_s$ . Due to the different velocities, the degeneracy is lifted and many more levels appear as the energy is increased (see also Fig. 4 in Ref. 8). Each level is classified by a spin and a charge quantum number  $m_s$  and  $m_c$ , respectively, which is reflected by the corresponding number of nodes and maxima in the wave functions. For example, the level  $m_s=4, m_c=1$  shows a superposition of two charge maxima and five weaker spin maxima. The integrated weight of the individual levels decreases with increasing energy, but the total (averaged) density of states increases with the known power law  $\rho(\omega) \propto \omega^{\beta_s^2 + \beta_c^2}$ . The superstructures survive even in the continuum limit and give rise to the observed slow oscillations with wave vectors  $\omega/v_c$  and  $\omega/v_s$  near the edge of a semiinfinite Luttinger liquid.<sup>8,9,11,12</sup> In the noninteracting limit  $g_s=g_c=1$ , we recover again standing waves with a fixed wave vector without any modulations, and remarkably all the many degenerate spin and charge bo-

son states at each energy level exactly sum up to an integrated normalized spectral weight of unity.

In Fig. 3 we have chosen values of  $g_s=0.7$  and  $g_c=0.6$ , which emphasize the locations of both spin and charge modulations, but in systems where the interactions are mostly spin independent  $g_s$  is likely to be much closer to unity and the spin modulations are less pronounced. Nonetheless, the level structure due to  $v_s < v_c$  as well as the charge modulations are likely to be observable when classifying Luttinger liquid systems in real space with STM experiments. In experimental systems there will be a number of complications that have to be taken into account. First of all in order to observe the features, the temperature has to be well below the characteristic energy scale  $\pi v_F/L$ , which corresponds to a few hundred degrees kelvin for a nanostructure of about 100 Å. Second, nonuniversal higher order operators in the field theory as well as long-range interactions may alter the behavior near the edges and give corrections to the depletion with the power law  $x^{2\alpha\beta}$ , although the node structure will be rather robust. Additional bands may also be observed by the STM at higher energies, which has to be

taken into account depending on the individual system. Carbon nanotubes are one promising system, but unfortunately in ordinary STM experiments the metallic substrate appears to screen all interaction effects,<sup>1-3</sup> while a less conducting surface may impede the quality of the STM images. Other possible systems include metallic one-dimensional nanostructures on cleaved surfaces<sup>13</sup> and cleaved edge overgrowth wires, where spectral properties can be detected indirectly by a clever way of analyzing the tunneling between adjacent wires as a function of voltage and magnetic field.<sup>14</sup> At this point we cannot speculate which experimental system is best suited, but given the rapid progress in STM imaging and nanostructured materials the predicted wave functions are likely to be observable soon when classifying different kinds of potential Luttinger liquid systems.

In conclusion we have shown that the single-particle wave functions of interacting fermions in a box can be used to visualize the true nature of the underlying boson excitations.

This research was supported in part by the Swedish Research Council and INFM.

<sup>1</sup>L.C. Venema, J.W.G. Wildoer, J.W. Janssen, S.J. Tans, H.L.J.T. Tuinstra, L.P. Kouwenhoven, and C. Dekker, *Science* **283**, 52 (1998).

<sup>2</sup>S.G. Lemay, J.W. Janssen, M. van den Hout, M. Mooij, M.J. Bronikowski, P.A. Willis, R.E. Smalley, L.P. Kouwenhoven, and C. Dekker, *Nature (London)* **412**, 617 (2001).

<sup>3</sup>Due to the metallic substrates, interaction effects are screened in the two experiments, Refs. 1,2.

<sup>4</sup>M.A. Cazalilla, *Europhys. Lett.* **59**, 793 (2002).

<sup>5</sup>F.D.M. Haldane, *J. Phys. C* **14**, 2585 (1981).

<sup>6</sup>For a compact review see D. Sénéchal, cond-mat/9908262 (unpublished).

<sup>7</sup>M. Fabrizio and A.O. Gogolin, *Phys. Rev. B* **51**, 17 827 (1995).

<sup>8</sup>A.E. Mattsson, S. Eggert, and H. Johannesson, *Phys. Rev. B* **56**, 15 615 (1997).

<sup>9</sup>S. Eggert, H. Johannesson, and A. Mattsson, *Phys. Rev. Lett.* **76**, 1505 (1996).

<sup>10</sup>C.L. Kane and M.P.A. Fisher, *Phys. Rev. Lett.* **68**, 1220 (1992).

<sup>11</sup>S. Eggert, *Phys. Rev. Lett.* **84**, 4413 (2000).

<sup>12</sup>V. Meden, W. Metzner, U. Schollwock, O. Schneider, T. Stauber, and K. Schonhammer, *Eur. Phys. J. B* **16**, 613 (2000).

<sup>13</sup>P. Segovia, D. Purdie, M. Hengsberger, and Y. Baer, *Nature (London)* **402**, 504 (1999).

<sup>14</sup>O.M. Auslaender, A. Yacoby, R. de Picciotto, K.W. Baldwin, L.N. Pfeiffer, and K.W. West, *Science* **295**, 825 (2002).